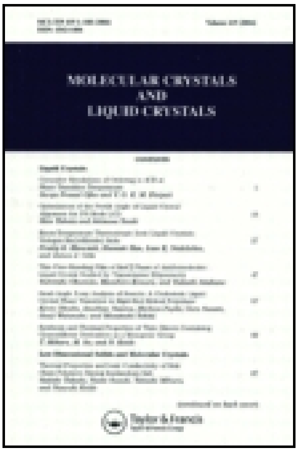

Molecular Crystals and Liquid Crystals
Publication details, including instructions for authors and subscription information:
http://www.tandfonline.com/loi/gmcl20

Fabrication and Characteristics of mc-Si Solar Cells with RIE-Textured Surface

Kwang Mook Park [a], Myoung Bok Lee [b], Ji Hee Jung [c] & Sie Young Choi [a]

[a] Graduate school of electrical engineering and computer science, Kyungpook National University, Daegu, 702-701, Korea

[b] Nano Fusion Development team, Daegu Technopark Nano Convergence Practical Application Center, Daegu, 704-801, Korea

[c] Green energy research division, Daegu Gyeongbuk Institute of Science and Technology, Daegu, 711-873, Korea

Version of record first published: 30 Aug 2012.

To cite this article: Kwang Mook Park, Myoung Bok Lee, Ji Hee Jung & Sie Young Choi (2012): Fabrication and Characteristics of mc-Si Solar Cells with RIE-Textured Surface, Molecular Crystals and Liquid Crystals, 565:1, 115-123

To link to this article: http://dx.doi.org/10.1080/15421406.2012.693289

Mol. Cryst. Liq. Cryst., Vol. 565: pp. 115–123, 2012

ISSN: 1542-1406 print/1563-5287 online
DOI: 10.1080/15421406.2012.693289

Fabrication and Characteristics of mc-Si Solar Cells with RIE-Textured Surface

KWANG MOOK PARK,[1] MYOUNG BOK LEE,[2,*]
JI HEE JUNG,[3] AND SIE YOUNG CHOI[1,*]

[1]Graduate school of electrical engineering and computer science, Kyungpook National University, Daegu 702-701, Korea
[2]Nano Fusion Development team, Daegu Technopark Nano Convergence Practical Application Center, Daegu 704-801, Korea
[3]Green energy research division, Daegu Gyeongbuk Institute of Science and Technology, Daegu 711-873, Korea

Reactive ion etching (RIE) texturing is well-known as an effective method to form the surface structure on a multi-crystalline (mc-Si) wafer that has grains with randomly oriented crystallites. The saw damage removal (SDR) process using HF/HNO$_3$/D.I (HND) solution was employed in this work, since the etching rate of RIE dry etching was lower than that of wet etching. The surface morphology on mc-Si surface was formed by RIE using a gas flow ratio of SF_6:O_2 = 1:1.22. The control of RF power and working pressure could etch the mc-Si surface of the 15.6 × 15.6 cm^2 area uniformly during RIE texturing process. The surface morphologies textured for 5 and 10 min were needle-like structures and sharp grass-like structures, respectively. Solar cells with the needle-like structure had higher values for open circuit voltage (V_{oc}), short circuit current (I_{sc}), fill factor (FF), and efficiency, despite higher reflectance compared to those with the sharp grass-like structure. The cell textured for 10 min was expected to have non-homogeneous emitter layer as the dark I-V curves of the cells textured for 5 and 10 min were compared.

Keywords RIE texturing; SDR; reflectance; needle-like structure; emitter layer

Introduction

The demand to develop mc-Si solar cells of low cost and high conversion efficiency to diminish the loss of incoming light at a mass production level has increased [1]. Study on surface texturing to induce multi-reflection has been widely conducted. Surface texturing of mc-Si is presently conducted by wet etching methods using surface texturing of mono-crystalline (c-Si). Specifically, the alkali etching method used to form random pyramidal structures at <100> c-Si is not very effective in texturing mc-Si due to grains with randomly orientated crystallites [1–3]. Therefore, various studies on effective surface texturing of mc-Si, such as mechanical methods, like sandblasting or dicing, laser grooving, acid etching and the plasma dry etching, have been attempted [4–6]. RIE, a kind of plasma dry etching

*Addressed correspondence to S.Y. Choi, Graduate School of Electrical Engineering and Computer Science, Kyungpook National University, Sangyuk-dong, Buk-gu, Daegu 702-701, Korea (ROK). Tel.: (+82)53-940-8618; Fax: (+82)53-950-6837. E-mail: sychoi@ee.knu.ac.kr

method, has gained wide-spread interest due to the formation of uniform structures, the contact free, the low consumption of Si and its fast, simple process. The Kyocera group, which published a special result of 17.1% efficiency for mc-Si solar cells textured by RIE using Cl_2 gas, demonstrated the feasibility of mass production [7]. The RIE texturing process using a gaseous mixture based on SF_6/O_2 has been studied recently due to the toxic characteristics of Cl_2 gas. SF_6/O_2 gas plasma is well-known to form an appropriate structure on the mc-Si surface without the process of patterning, since SF_6/O_2 gas plasma at the critical condition can form volatile silicon oxyfluoride (SiO_xF_y) on the mc-Si surface that can generate selective etching during the RIE texturing process [4,6,8,9]. However, the RIE process using SF_6/O_2 gas plasma has not yet had reports to clearly improve conversion efficiency.

In this work, we study RIE texturing using SF_6/O_2 gas to form uniform structures at 15.6 × 15.6 cm^2 mc-Si surface and to decrease the average reflectance. First, the HND etching process was employed to remove the saw damage of the mc-Si surface and the etching characteristics were investigated. Second, RIE texturing, which aimed at determining the lowest reflectance and uniform structures, was conducted. We analyzed the interaction among surface morphology, reflectance, and electrical characteristics after the RIE texturing process. Finally, the mc-Si solar cells with the textured surface were fabricated and their electrical properties were characterized by analysis of the dark I-V, conversion efficiency, and external quantum efficiency (EQE).

Experiment and Measurements

2.1. SDR

The volume ratio of HND was $HF:HNO_3:D.I = 1:2.7:3$ for the SDR process with an etching time of 2 min. The surface structure after the SDR process was observed using FE-SEM. The etching depth was calculated after measuring the weight of mc-Si before and after HND etching. The minority carrier lifetime and reflectance were measured.

2.2. RIE Texturing

The RIE texturing process using SF_6/O_2 mixtures targets the minimized average reflectance and uniform structures by controlling parameters, such as RIE power, total gas flow rate, ratio of gases, etching time, working pressure, and the gap between the top and bottom electrodes. The desirable amount of texturing was achieved when the process parameters were RIE power (frequency of 12.56 MHz) of 75 W, working pressure of 32 mTorr, and SF_6/O_2 gas mixture applied. The wafers used in texturing process were SOG mc-Si wafers with specifications of a sheet resistance of 1.4∼1.6 Ω·cm, lifetime above 1.5 μs, 200 μm thick, p-type doped boron, and size 15.6 × 15.6 cm^2. As-cut mc-Si wafers with the same grain group were used to enhance the reliability of the experiment. The reflectance for wavelengths ranging from 310 to 1100 nm and minority carrier lifetime were measured. The surface morphologies for the minimized average reflectance were observed using FE-SEM.

2.3. Fabrication of mc-Si Solar Cells With Textured Surface

The fabrication process for the solar cells is described as follows. The surface texturing process was conducted in the first step after SDR. Then, an emitter layer was formed by a conventional pre-deposition and diffusion process using an H_3PO_4 solution. Phosphorus silica glass (PSG) was removed and the silicon nitride layer about 80∼85 nm thick was deposited by plasma enhanced chemical vapor deposition (PECVD). The front and back electrode was formed using a screen printing method, followed by a co-fire process for the back surface field (BSF), metallization and silicon nitride contacts. The solar cells with textured surface were finished after edge isolation. The performance parameters and EQE of the fabricated solar cells were measured to examine the correlation between the surface morphologies and the electrical properties.

Results and Discussion

Saw damage on the mc-Si surface generated during the wire sawing process revealed that the performance parameters of solar cells degenerated. Wet etching methods have been employed to remove the saw damage of the mc-Si surface. In this work, an HND solution with an isotropic characteristic, among these wet etching methods, was employed, since the alkali etching was inappropriate to mc-Si that consists of grains with randomly oriented crystallites. The overall etching process of HND solution is initiated by autocatalysis of HNO_3. The cathodic reduction of HNO_3 results in an oxidation reaction by a supply of holes and then HF dissolves the formed SiO_2 by forming soluble complex H_2SiF_6. This process is represented by the following reaction equation [3];

$$Si + HNO_3 + 6HF = H_2SiF_6 + HNO_3 + H_2O + H_2$$

An HND solution with a volume ratio of $HF{:}HNO_3{:}D.I = 1{:}2.7{:}3$ was used and mc-Si wafers were dipped in an HND solution for 2 min. The average reflectance and etching depth for a volume ratio of $HF{:}HNO_3{:}D.I = 1{:}2.7{:}3$ were about 27.6% and 3.8 μm, respectively. Figure 1 shows the surface morphology after SDR. Pore-like structures with a smooth and rounded surface were observed and their average width and depth were about 5∼10 μm and about 2∼3 μm, respectively.

The RIE texturing process using gas flow ratios of $SF_6{:}O_2 = 1{:}1.5$, 1:1.35, 1:1.22, and 1:1.1 was conducted for 5 min; then, the surface reflectance for RIE texturing using different gas volume ratios was analyzed. Figure 2 represents the reflectance for wavelengths between 310 and 1100 nm for each sample after RIE texturing. The average reflectance for gas flow ratios of $SF_6{:}O_2 = 1{:}1.5$, 1:1.35, 1:1.22, and 1:1.1 were 37.3, 27.3, 13.2, and

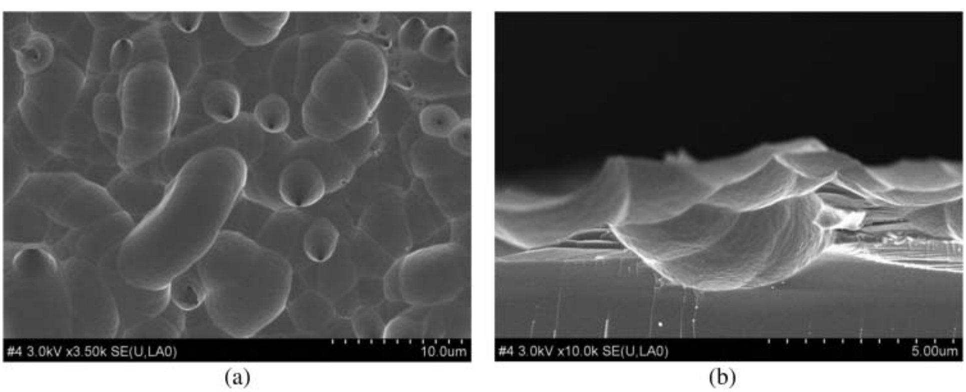

Figure 1. FE-SEM image of mc-Si surface after SDR using acid etching with a volume ratio of $HF{:}HNO_3{:}D.I. = 1{:}2.7{:}3$. (a) Top view; (b) Cross view.

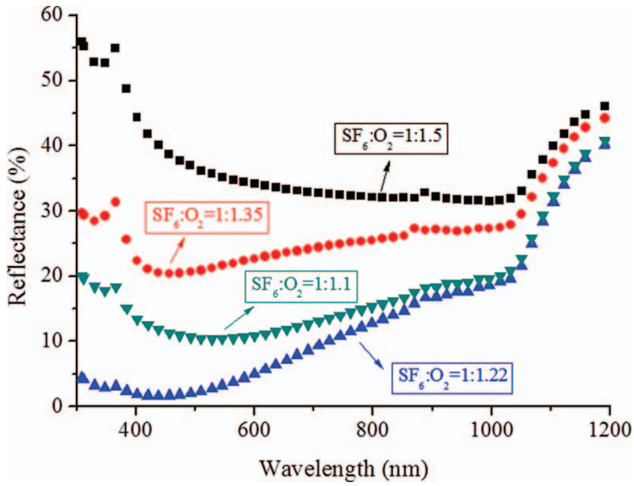

Figure 2. Reflectance spectrum of mc-Si textured with four different gas volume ratios of SF_6/O_2 gas.

18.2%, respectively, under the same etching time of 5 min. The more the oxygen ratio decreased, the more the reflectance gradually decreased until 13.2%, with the exception of the reflectance for $SF_6:O_2 = 1:1.11$, at which the reflectance increased again. The minimized average reflectance was obtained at a gas flow ratio of $SF_6:O_2 = 1:1.22$ for 5 min RIE texturing. This characterized that the reflectance for the wavelength in the range of 310∼550 nm sharply decreased, more than the reflectance for the wavelength in the range of 850∼1100 nm. RIE texturing under varying SF_6/O_2 gas flow ratios could effectively decrease the amount of reflectance for short wavelengths. Figure 3 shows the variation of average reflectance based on texturing time. The average reflectance decreased about 4% per minute, except for a RIE texturing time of 1 min, so the average reflectance for

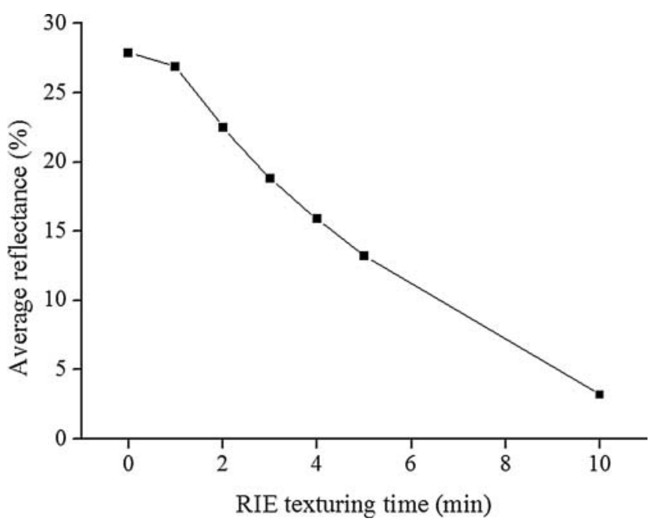

Figure 3. Variation of average reflectance of RIE-textured mc-Si at a gas flow ratio of $SF_6:O_2 =$ 1:1.22 as a function of RIE texturing time.

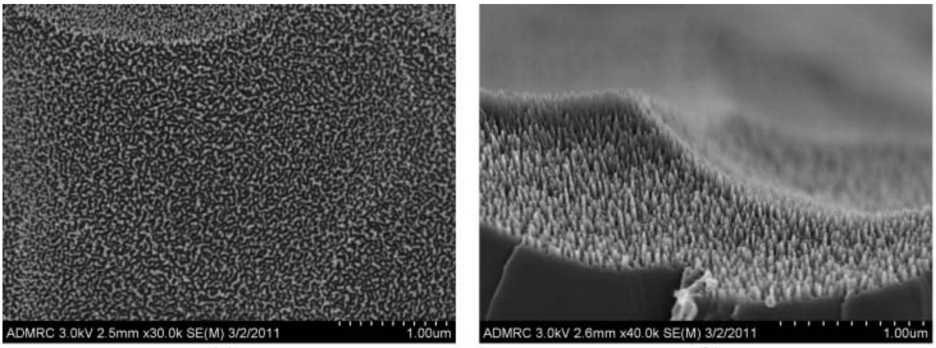

(a) (b)

Figure 4. FE-SEM image of mc-Si surface textured at a gas flow ratio of SF_6:O_2 = 1:1.22 for 5 min. (a) Top view; (b) Cross view.

the RIE texturing time between 0 and 5 min decreased from 27.9 to 13.2%. The average reflectance could be decreased by 3.2% when RIE texturing was conducted for 10 min. These results indicated that the surface morphology inducing multi-reflection for incoming light was governed by the SF_6/O_2 gases flow ratio and texturing time. In the critical SF_6/O_2 gases flow ratio, the O* radical in the critical SF_6/O_2 volume ratio partially creates volatile SiO_xF_y on the Si surface. The SiO_xF_y helps control etching profiles, since it induces non-homogeneous etching and side wall passivation during RIE texturing [8,11,12]. Thus, specific structures on the mc-Si surface were formed by such non-uniform etching. The sidewall passivation formed by the SiO_xF_y would be sensitive to the oxygen content at the silicon surface; whereas, both the deficiency and oversupply of oxygen caused a polished surface for mc-Si. The small oxygen content would increase the etching rate, since it helps to separate the F* radical from the SF_6 gas and too much oxygen content could not take the place of the F* radical efficiently. RF power and working pressure both affected formation of uniform surface structures on 15.6 × 15.6 cm^2 size. The variation of RF power and working pressure were related to the etching rate of the central portion and the edge portion of the mc-Si wafer, respectively. An RF power above 100 W decreased the reflectance of the central portion more than that of the edge portion. In a high working pressure above 50 mTorr, the reflectance of the edge portion decreased more than that of the central portion,

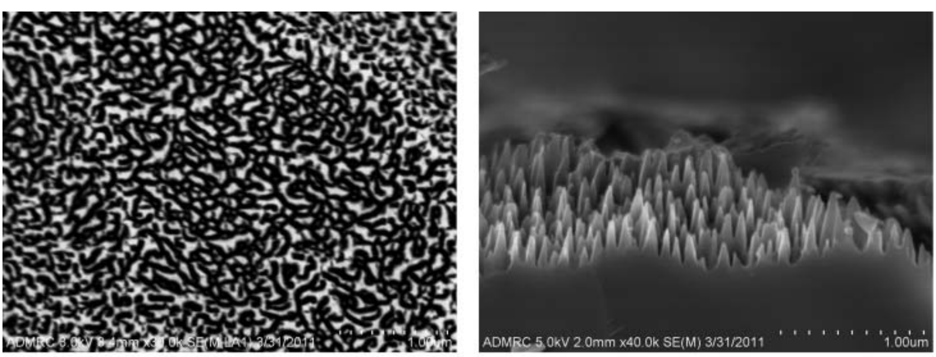

(a) (b)

Figure 5. FE-SEM image of mc-Si surface textured at a gas flow ratio of SF_6:O_2 = 1:1.22 for 10 min (a) Top view; (b) Cross view.

even though more radicals might be produced. The edge of a square would exhibit non-uniform etching, since it caused the power to concentrate. Therefore, uniform reflectance could be obtained by controlling the RF power and the working pressure, regardless of wherever the reflectance was measured. Figures 4 and 5 show the surface morphologies after RIE texturing conducted at SF_6:O_2 = 1:1.22 for 5 and 10 min, respectively. The surface morphology textured for 5 min had needle-like structures with diameters ranging from 30 to 50 nm with heights from 100 to 150 nm. The surface morphology textured for 10 min was close to the sharp grass-like structure. The width of the bottom side and height were about 60 to 80 nm and 200 to 250 nm, respectively. When the RIE texturing time was extended two times, the width and height of the structures also increased about two times and the gaps between the structures increased. We noticed that a surface morphology with appropriate gaps between the structures and sufficient height to induce effective multi-reflection was needed to lower the reflectance further.

The WT-2000PV was used to measure the average minority carrier lifetime of the textured mc-Si. This technique is based on the generation and the recombination of carriers. The pulse of an infrared semiconductor laser generates free electron-hole pairs under the illuminated area on a sample. The free electrons' concentration and the conductivity of the sample decrease after the excitation, since the free electrons and holes recombine. The decaying conductivity can be monitored by detecting the microwave reflectivity, because the reflected microwave power is proportional to the conductivity of the sample. Figure 6 shows the variation of average lifetime according to the process step when RIE texturing was conducted at a gas flow ratio of SF_6/O_2 = 1:1.22 for 10 min. Although the lifetime after SDR was increased, the one after RIE texturing was as low as for bare mc-Si. The lifetime after depositing ARC was about 2.5 times more than that of bare mc-Si. Although the lifetime for the ARC slightly increased, it was still characterized as having a low value. This indicates that the silicon nitride as ARC deposited using PECVD might not be able to sufficiently passivate the textured surface due to the rough surface and many surface defects created by plasma damage. Consequently, the effects could be summarized by stating that RIE texturing could effectively lower the loss of incoming light but the

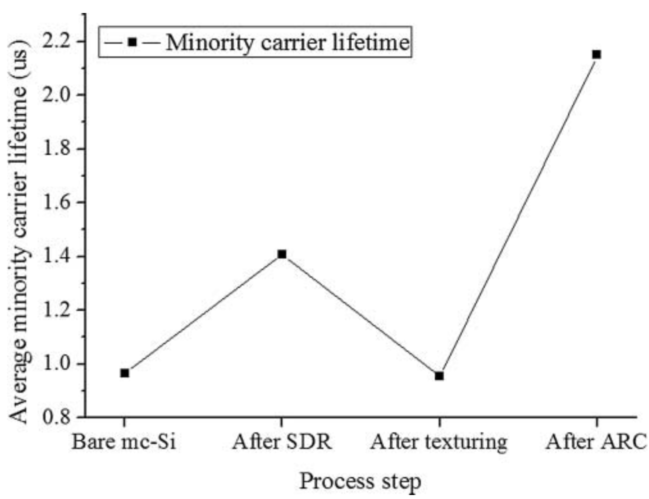

Figure 6. Variation of average minority carrier lifetime for process step.

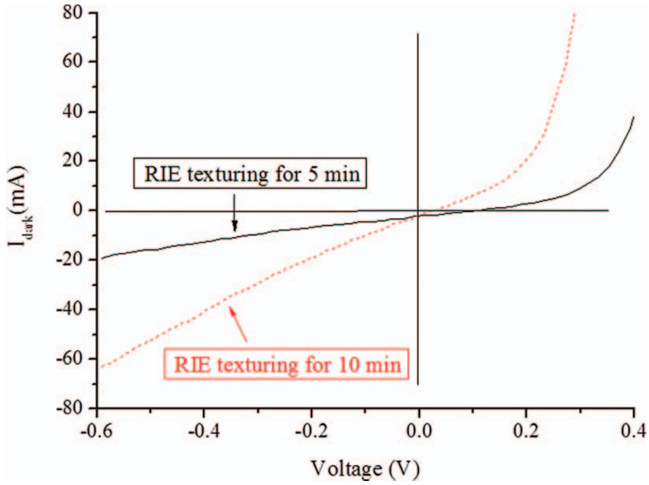

Figure 7. Comparison of dark I-V characteristics for mc-Si solar cells textured for 5 and 10 min.

efficiency of separation and collection for the excess carrier generated by incoming light were degraded due to surface defects and the rough surface structure.

Solar cells with their surface textured by RIE for 5 and 10 min were fabricated. Figure 7 represents the dark I-V characteristics of the fabricated solar cells. In solar cells textured for 10 min, large diode leakage current was three times larger compared to the other leakage current. Such a large leakage current was expected to cause low shunt resistance, so conversion efficiency would degenerate. This implied that the sample textured for 10 min could not form the stable pn junction, since surface impurities by siliconoxyflouride and the sharp structures formed during RIE texturing would keep from diffusing pentavalent impurity uniformly. Figure 8 represents the illuminated current-voltage characteristics of mc-Si solar cells with their surface textured for 5 and 10 min. The performance of cells was measured under the standard 100 mW/cm^2, AM1.5G at 25°C. The performance parameters

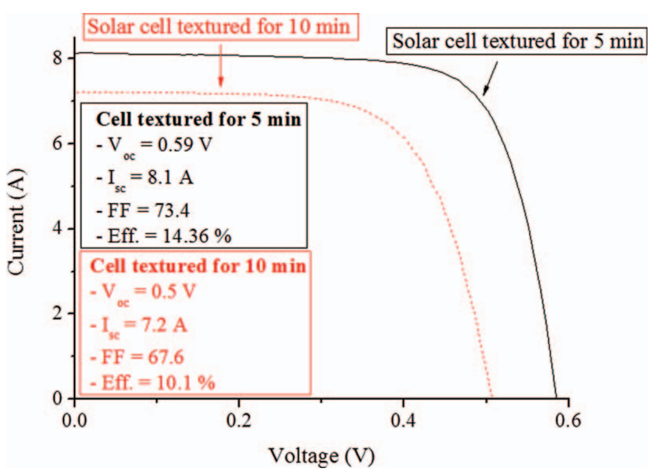

Figure 8. Comparison of light I-V characteristics for mc-Si solar cells textured for 5 and 10 min.

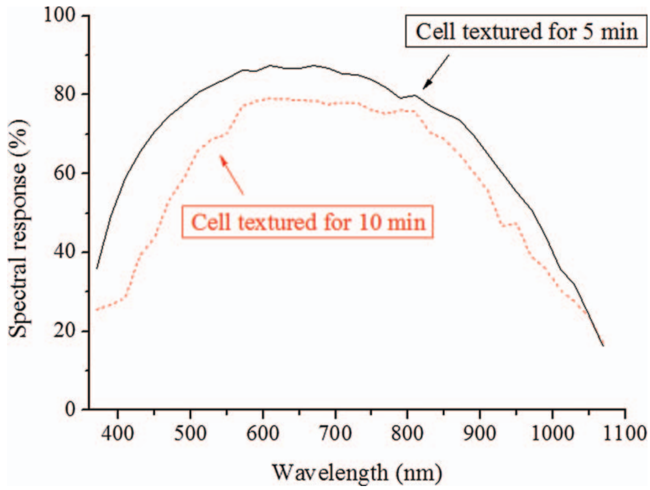

Figure 9. Comparison of EQE for mc-Si solar cells textured for 5 and 10 min.

of cells textured for 5 min were significantly higher than those of cells textured for 10 min. The open circuit voltage (V_{oc}) and short circuit current (I_{sc}) of the cells textured for 5 and 10 min were about 0.59 V and 8.1 A, and about 0.5 V and 7.2 A, respectively. Consequently, the conversion efficiency for cells textured for 10 min were less 4.26% than that for 5 min. As the reflectance decreased, the increased I_{sc} was expected, since the RIE textured cells could absorb much more light to generate the electron-hole pair (EHP) in the cell. However, contrary to our expectation, all the performance parameters of the cell degraded with extended texturing time. Although the RIE texturing time of 10 min could lower the loss of incoming light, it could not improve the efficiency. This might be due to surface impurity and surface morphology disturbing the doping process. The EQE shown in Figure 9 supports the results for the performance parameters of solar cells with different process times. It shows that the spectral response of EQE for cells textured for 10 min are less than that for 5 min in the range from 370 to 1100 nm. The best response of cells textured for 5 and 10 min were about 87% and 79% between 600 and 700 nm, respectively. The cause of the low electrical characteristics for RIE textured cells were generally accepted to be surface defects, the non-homogeneous emitter layer, contact resistance between the electrode and Si surface, and so on. In our work, the non-homogeneous emitter layer was considered the main cause of the low electrical characteristics of the cells textured for 10 min, as the result of the dark I-V characteristics and EQE were analyzed. In view of the results thus far, we realized we need to trade-off between the decrease of the surface reflectance and the improvement of electrical characteristics of mc-Si by forming the stable emitter layer.

Conclusion

RIE texturing has been performed on mc-Si wafers after the SDR process. The appropriate texturing conditions have been investigated for application to mc-Si solar cells. A minimized average reflectance of about 3.2% was obtained when RIE texturing with a gas flow ratio of $SF_6:O_2 = 1:1.22$ was conducted for 10 min. The minority carrier lifetime after RIE texturing was as low as the lifetime of bare mc-Si and the lifetime of the sample after depositing

ARC was increased about 2.5 times compared to that of RIE textured mc-Si. The surface morphologies textured for 5 and 10 min were needle-like structures and sharp grass-like structures, respectively. The width of the bottom side and height of surface morphology textured for 10 min were two times larger than that textured for 5 min. The conversion efficiency of solar cells with their surface textured for 5 and 10 min were 14.36 and 10.1%, respectively. When the dark I-V characteristics of both solar cells were compared, the cell textured for 10 min was expected to have a non-homogeneous emitter layer. We would need to balance the decrease of the surface reflectance and the degeneration of electrical characteristics of mc-Si to improve the performance parameters of solar cells further.

Acknowledgment

This research was financially supported by the Ministry of Knowledge Economy (MKE), Korean Institute for Advancement of Technology (KIAT) and Dae-Gyeong Leading Industry Office through the Leading Industry Development for Economic Region

References

[1] Lee, J. H. (2005). *Principle of solar cell*, HongRung publishing company: Seoul, p. 281.
[2] Gonzalez-Diaz, B., Guerrero-Lemus, R., Diaz-Herrera, B., Marrero, N., Mendez-Ramos, J., & Borchert, Dietmar (2009). *Mater. Sci. Eng. B*, *159–160*, 295.
[3] Kim, K. H., Dhungel, S. K., Jung, S. W., Mangalaraj, D., & Yi, J. (2008). *Sol. Energy Mater. Sol. cells*, *92*, 960.
[4] Yoo, J. S., Parm, I. O., Gangopadhyay, U., Kim, Kyunghae, Dhungel, S. K., Mangalaraj, D., & Yi, Junsin (2006). *Sol. Energy Mater. Sol. Cells*, *90*, 3085.
[5] Dekkers, H. F. W., Duerinckx, F., Szlufcik, J., & Nijs, J. (2000). *Opto-electron. Rev.*, *8*(4), 311.
[6] Kumaravelu, G., Alkaisi, M. M., Bittar, A., Macdonald, D., & Zhao, J. (2004). *Curr. Appl. Phys*, *4*, 108.
[7] Inomata, Y., Fukui, K., & Shirasawa, K. (1997). *Sol. Energy Mater. Sol. Cells*, *48*, 237.
[8] Kumaravelu, G., Alkaisi, M.M., & Bittar, A. (2002). in: *Proceedings of the 29th IEEE Photovoltaic Specialists Conference*, p. 259.
[9] Yoo, J. S., Yu, G. J., & Yi, J. S. (2011). *Sol. Energy Mater. Sol. Cells*, *95*, 2.
[10] Gangopadhyay, U., Dhungel, S. K., Basu, P. K., Dutta, S. K., Saha, H., & Yi, J. (2007). *Sol. Energy Mater. Sol. Cells*, *91*, 285.
[11] Jansen, H., de Boer, M., Wensink, H., Kloeck, B., & Elwenspoek, M. (2001). *Microelectron. J.*, *32*, 769.
[12] Jansen, H., de Boer, M., & Elwenspoek, M. (1996). in: *IEEE, Micro Electro Mechanical Systems*, MEMS' 96, Proceedings, San Diego, CA, p. 250.